AtHMA1 Is a Thapsigargin-sensitive Ca^{2+}/Heavy Metal Pump*

Ignacio Moreno[‡], Lorena Norambuena[§], Daniel Maturana[‡], Mauricio Toro[¶], Cecilia Vergara[‡], Ariel Orellana[‖], Andrés Zurita-Silva[¶], and Viviana R. Ordenes[‡¶1]

From the [¶]Laboratorio de Biología Molecular Vegetal, Centro de Estudios Avanzados en Zonas Áridas (CEAZA), La Serena 1720170, Chile, [‡]Laboratorio de Fisiología Celular, Facultad de Ciencias, Universidad de Chile, Santiago 7800024, Chile, [§]Laboratorio de Biología Molecular Vegetal, Facultad de Ciencias, Universidad de Chile, Santiago 1720170, Chile, and [‖]Millenium Nucleus in Plant Cell Biotechnology, Centro de Biotecnología Vegetal, Universidad Andrés Bello, Santiago 8370146, Chile

The *Arabidopsis thaliana* AtHMA1 protein is a member of the P_{IB}-ATPase family, which is implicated in heavy metal transport. However, sequence analysis reveals that AtHMA1 possesses a predicted stalk segment present in SERCA (sarcoplasmic/endoplasmic reticulum Ca^{2+} ATPase)-type pumps that is involved in inhibition by thapsigargin. To analyze the ion specificity of AtHMA1, we performed functional complementation assays using mutant yeast strains defective in Ca^{2+} homeostasis or heavy metal transport. The heterologous expression of AtHMA1 complemented the phenotype of both types of mutants and, interestingly, increased heavy metal tolerance of wild-type yeast. Biochemical analyses were performed to describe the activity of AtHMA1 in microsomal fractions isolated from complemented yeast. Zinc, copper, cadmium, and cobalt activate the ATPase activity of AtHMA1, which corroborates the results of metal tolerance assays. The outcome establishes the role of AtHMA1 in Cd^{2+} detoxification in yeast and suggests that this pump is able to transport other heavy metals ions. Further analyses were performed to typify the active Ca^{2+} transport mediated by AtHMA1. Ca^{2+} transport displayed high affinity with an apparent K_m of 370 nM and a V_{max} of 1.53 nmol mg^{-1} min^{-1}. This activity was strongly inhibited by thapsigargin (IC_{50} = 16.74 nM), demonstrating the functionality of its SERCA-like stalk segment. In summary, these results demonstrate that AtHMA1 functions as a Ca^{2+}/heavy metal pump. This protein is the first described plant P-type pump specifically inhibited by thapsigargin.

Plant Ca^{2+} and heavy metal-ATPases belong to the superfamily of P-ATPases (1, 2). Their common characteristic is the presence of a phosphorylated intermediary in the catalytic cycle. In *Arabidopsis*, the heavy metal-ATPases belong to the P_{IB} subfamily and normally have eight predicted transmembrane domains, whereas the Ca^{2+}-ATPases are part of the P_{IIA} and P_{IIB} subfamilies and have ten predicted transmembrane domains (2). A common feature among the P_{IB}-ATPases is the presence of a CP*X* motif, which is though to play a role in metal translocation, as well as putative metal-binding domains located at the amino or carboxyl terminus (3). On the other hand, P_{IIB} ATPases have a calmodulin-binding domain that regulate their activity; however, the P_{IIA} do not have this domain (4). The most important difference between the calcium and heavy metal-ATPases is their substrate specificity (1). However, *in vitro* metal transport studies performed with membrane fractions isolated from seedlings suggest that one or more members of the superfamily of P-ATPases are capable of transporting calcium and heavy metals. The studies showed competitive inhibition between active transport of heavy metals (such as copper and cadmium) and calcium.[2] Interestingly, both transport activities were inhibited by the sesquiterpene lactone thapsigargin, a potent and specific inhibitor of SERCA[3]-type pumps (5–7). To date no one has described plant ion pumps that transport calcium and heavy metals in biochemical terms, nor have scientists described genes encoding for ion pumps inhibited by thapsigargin or plant mutants with thapsigargin-sensitive/tolerant phenotypes. Based on the results of biochemical assays suggesting the existence of thapsigargin-sensitive Ca^{2+}/heavy metal-ATPase, we searched for potential candidate proteins in the *Arabidopsis* genome. This was made possible by the highly conserved "stalk segment" or S3 sequence adjacent to the third transmembrane segment of the SERCA pumps (8, 9) composed of amino acids DEFGEQLSK (5–7). This sequence was almost complete and was annotated as a stalk segment (using the topology prediction software ARAMEMNON) in the *Arabidopsis* heavy metal pump AtHMA1 (At4g37270). This pump belongs to the subclass of zinc/cobalt/cadmium/lead-ATPases and is the most divergent metal pump of the *Arabidopsis* P_{IB}-ATPases (1, 2, 10, 11) (see Fig. 1). It lacks an amino-terminal heavy metal-binding domain, such as *GMXCXXC* or GICC(T/S)SE, which is often found in other members of the group. It has an intramembranous SPC instead of the CP(C/H/S) motif located at the putative metal transporting site of P_{IB}-ATPases (11, 12). The pump possesses other structural characteristics related to heavy metal binding and transport, such as a poly-H motif commonly found in zinc-binding proteins, several C and CC pairs, and a HP

* This work was supported mainly by Fondo Nacional de Desarrollo Científico y Tecnológico (FONDECYT) Grant 3040057 and in part by FONDECYT Grant 1040681 and by Grant PCB P06-065-F from Millennium Nucleus in Plant Cell Biology. The costs of publication of this article were defrayed in part by the payment of page charges. This article must therefore be hereby marked "*advertisement*" in accordance with 18 U.S.C. Section 1734 solely to indicate this fact.

[1] To whom correspondence should be addressed: Laboratorio de Biología Molecular Vegetal CEAZA, Universidad de La Serena, Campus Andres Bello, Casilla 599, La Serena 1720170, Chile. Tel.: 56-51-334855; Fax: 56-51-334741; E-mail: viviana.ordenes@ceaza.cl.

dipeptide (11, 12). Initial studies performed by Higuchi and Sonoike (13) show that an *Arabidopsis* disruption mutant of AtHMA1 is sensitive to high concentrations of zinc. Recently, it was demonstrated that AtHMA1 is localized in the chloroplast envelope, and *Arabidopsis* insertional mutants exhibit a lower chloroplast copper content and a diminution of the total chloroplast superoxide dismutase, activity suggesting a role for AtHMA1 in copper homeostasis (14). At this point, two key questions about the functions and ion specificities of AtHMA1 must be addressed. (i) Can AtHMA1 transport Ca^{2+}? (ii) In which heavy metal homeostatic mechanisms is AtHMA1 involved? We expressed AtHMA1 in yeast (*Saccharomyces cerevisiae*) in order to perform functional complementation assays. We demonstrated that AtHMA1 complements the mutant phenotype displayed by two Ca^{2+} transport-deficient yeast strains. *In vitro* calcium transport assays showed that AtHMA1 promotes thapsigargin-sensitive Ca^{2+} transport. AtHMA1 also complements a Cd^{2+}-hypersensitive yeast mutant and confers high Cd^{2+} tolerance onto wild-type yeast. Cadmium-stimulated ATPase activity of AtHMA1 confirms that this pump plays a role in cadmium transport. Expression of AtHMA1 also confers high zinc, copper, and cobalt tolerance onto yeast, and ATPase activity is also stimulated by the addition of these metals. Taken together, our results strongly suggest that AtHMA1 is a metal pump capable of transporting a wide range of ions including calcium. As such, AtHMA1 may represent a key element in the mechanism used to overcome ion deficiency or toxicity in *Arabidopsis thaliana*.

EXPERIMENTAL PROCEDURES

Cloning of AtHMA1—Full-length AtHMA1 cDNA (2460 bp) was supplied by RIKEN (15, 16). It was amplified using AccuTherm™ DNA polymerase (GeneCraft) and primers flanking the coding region designed from the genomic sequence At4g37270. Primer sequences were as follows: 5′-CGCTTG-AGATCTAATTCGTCGACCATGGAA-3′ (sense, BglII restriction site underlined) and 5′-AGACAAGCGGCCGC-AAGTTACCCCCTAATG-3′ (antisense, NotI restriction site underlined). After verification by sequencing, the amplification product was digested with BglII and NotI and ligated into BamHI/NotI-digested pGPD426, a uracil yeast (*S. cerevisiae*) expression vector (17) to generate pGPD426-AtHMA1. *Escherichia coli* strain DH5α was used to build and maintain plasmid stocks using standard molecular biology procedures (18).

Yeast Strains and Growth Conditions—The following *S. cerevisiae* strains were used in this study: YR98 (MATα, ade2 his3-Δ200 leu2-3,112 lys2-Δ201 ura3-52) and its isogenic mutant Δ*pmr1* (YR122) (pmr1-Δ1::Leu2); W303 (MATa, ade2-1 can1-100 his3-11,15 leu2-3,112 trp1-1 ura3-1) and its isogenic mutant K616 (pmr1::His3 cnb1::Leu2 pmc1::Trp1); and DTY165 (MATα, ura3-52 leu2-3,112 his3-Δ200 trp1-Δ901 lys2-801 suc2-Δ9) and its isogenic mutant Δ*ycf1* (DTY167) (ycf1::HisG). All strains were propagated at 30 °C in rich YPD medium, except K616, which was grown in YPD medium (1% (w/v) bacto-yeast extract, 2% (w/v) bacto-peptone, and 2% (w/v) glucose) supplemented with 10 mM $CaCl_2$ (19). Yeast transformation was performed using the LiAc method (20). After transformation, yeast cells were grown in a selective medium (0.67% yeast nitrogen base without amino acids, 2% glucose) and supplemented with appropriate auxotrophic requirements. Uracil-based selection was used to screen for transformants.

Expression of AtHMA1 in Yeast—AtHMA1 expression in transformed yeast was verified using RT-PCR. Transformed yeast was grown on a selective medium until an A_{600} of 0.6. Cells were then collected by centrifugation and used to isolate total RNA following the Chomczynski phenol-chloroform extraction method (21). The first strand of cDNA was prepared using a RevertAid™ first strand cDNA synthesis kit (Ferrmentas) with oligo(dT) and 1 μg of total RNA. After reverse transcription of mRNA to cDNA, a 565-bp fragment of the AtHMA1 cDNA was amplified by PCR using the following primers: 5′-ATGATGTTAACTGGGGACC-3′ (sense) and 5′-CTAAT-GTGCAGAGCTTAAACTGTTGCTGCTGCTACT-3′ (antisense). Amplification of ACT1 cDNA was used as an internal control in all reactions (22). The PCR products were separated by agarose gel electrophoresis.

Functional Complementation Assays—Functional complementation of Ca^{2+} transport-defective mutants K616 and Δ*pmr1* was carried out as described previously (19). Mutant and wild-type yeast strains transformed with pGPD426 or pGPD426-AtHMA1 were streaked onto growth plates lacking uracil and supplemented with 10 mM EGTA. Ca^{2+}-depleted plates were then incubated for up to 3 days at 30 °C. For functional complementation of the cadmium-hypersensitive yeast mutant Δ*ycf1*, the complementation was carried out by streaking transformed yeast onto growth plates lacking uracil and supplemented with 70 μM $CdCl_2$. High Cd^{2+} plates were incubated for up to 5 days at 30 °C.

Metal Toxicity Tests—To test sensitivity to high cadmium concentrations in Δ*ycf1* yeast transformed with AtHMA1, cells grown to log phase were diluted to an A_{600} of 0.1 and incubated in the presence of 70–200 μM $CdCl_2$. Growth at 30 °C was monitored by the change in A_{600} every 3 h for 21 h, and the rate of exponential growth of yeast cultures was expressed as generation time in hours, *i.e.* the doubling time of each yeast population. Sensitivity to other transition metals was tested by growing transformed Δ*ycf1* on solid media supplemented with 6 mM $CoCl_2$, 4 mM $CuSO_4$, or 28 mM $ZnCl_2$. Plates were incubated for 5 days at 30 °C. Additionally, the capacity of AtHMA1 to confer cadmium tolerance to wild-type yeast (W303) was tested by growing transformed cells in liquid medium with 70–200 μM $CdCl_2$, and the A_{600} of cultures was followed for 5 days.

Carboxypeptidase Y (CPY) Detection Assay—Transformed K616 and wild-type cells were grown in 3 ml of selective medium for 2 days at 30 °C. To obtain yeast lysate samples, cells were resuspended in 200 μl of SUMEB buffer (1% SDS, 8 M urea, 10 mM MOPS, pH 6.8, 10 mM EDTA, and 0.01% bromphenol blue) plus 100 μl of 500-μm glass beads (Sigma) and then vortexed three times for 1 min. The mixture was incubated for 10 min at 65 °C and centrifuged at 2,000 × *g*. The supernatant was collected. Two μl of supernatant (or yeast lysate) and 600 μl of growth media were transferred simultaneously onto a nitrocellulose membrane using a dot-blot device (Bio-Rad). The membrane was then washed briefly with water and blocked with 5% milk in TBS (10 mM Tris-HCl, pH 7.5, 150 mM NaCl, 0.1% Tween 20). Secreted CPY was detected by monoclonal anti-

CPY antibody (1:1,000) (Molecular Probes). Anti-mouse IgG antibody-horseradish peroxidase conjugate (1: 10,000; Molecular Probes) was used as secondary antibody.

Isolation of Yeast Membranes—Membranes were prepared from yeast cells as described previously (23). 2–5 ml of stationary phase cultures of transformed yeast was diluted into 300 ml of appropriate selective medium, grown for 24 h at 30 °C to an A_{600} of ~0.8, and collected by centrifugation. After being washed with distilled water, the cells were resuspended in 1 volume of a buffer solution containing 10% sucrose, 25 mM Hepes-bis-Tris propane, pH 7.5, 2 mM $MgCl_2$, 2 mM dithiothreitol, 1 mM EGTA, and a mixture of protease inhibitors (1 mg/ml aprotinin, 1 mg/ml leupeptin, 1 mg/ml pepstatin, and 1 mM phenylmethylsulfonyl fluoride). One volume of 500-μm glass beads was added to the mixture, and yeast cells were disrupted by vortexing at maximum speed for 2 min. The homogenate was centrifuged at 5,000 × *g* for 5 min at 4 °C. The supernatant was collected and centrifuged at 110,000 × *g* for 1 h. The resulting pellet was resuspended in 200 μl of a buffer solution containing 10% sucrose, 20 mM Hepes-bis-Tris propane, pH 7.0, 1 mM dithiothreitol, and the mixture of protease inhibitors described above. The membrane preparations were aliquoted and stored at −80 °C until needed. Protein content was measured using the bicinchoninic acid method (Pierce Chemical) with bovine serum albumin as standard.

ATPase Activity Assays—These assays were carried out as described previously (24). Yeast vesicles (50 μg protein/ml) were mixed with a reaction buffer containing 50 mM Tris, pH 7.5, 3 mM $MgCl_2$, 3 mM ATP, 20 mM Cys, 1 mM dithiothreitol, and each metal (at 1 μM) listed in Fig. 6*A*. The reaction mixture was incubated for 15 min at 30 °C. Released inorganic phosphate was determined colorimetrically (25). Background activity measured in the absence of metals was less than 10% of the highest metal-stimulated activity and was subtracted from the activity determined in the presence of metals. The results are the average of four independent experiments with measurements performed in triplicate. The relative activity was standardized by setting the highest value obtained from the measurements (48.15 nmol μg^{-1}) at 100% relative activity. All subsequent values were then adjusted accordingly and the S.E. was calculated.

$^{45}Ca^{2+}$ Uptake Assays—Ca^{2+} uptake by membranes of transformed yeast was assayed measuring $^{45}Ca^{2+}$ accumulation using the filtration method (26). Membrane samples were suspended (0.3–0.6 mg protein/ml final concentration) in a reaction buffer (3 ml) containing 250 mM sucrose, 25 mM Hepes-bis-Tris propane (pH 7.0), 10 mM KCl, and 0.4 mM NaN_3. Free Ca^{2+} concentration in the reaction buffer was set at desired values using variable amounts of $^{45}CaCl_2$ (containing 2.4 Ci of $^{45}Ca^{2+}$ $mmol^{-1}$ $CaCl_2$, PerkinElmer Life Sciences) and EGTA. Free Ca^{2+} concentrations were calculated using the WinMaxC 2.05 computer program. Vesicles were incubated in the buffer at 25 °C for 1 min, and transport was initiated (time zero) by adding a mixture of ATP and $MgCl_2$ to final concentrations of 2 and 3 mM, respectively. Samples of 200 μl were taken at different times and filtered through 0.45-μm nitrocellulose membranes (Millipore, Bedford, MA). The filters were rinsed immediately with 5 ml of ice-cold STOP buffer containing 250 mM sucrose, 2.5 mM Hepes-bis-Tris propane, pH 7.0, and 0.2 mM $CaCl_2$. The $^{45}Ca^{2+}$ radioactivity associated with the filters was determined by liquid scintillation counting. Ca^{2+} uptake was expressed as nmol Ca^{2+}/mg protein in the presence and absence of ATP-Mg. To determine the K_m for Ca^{2+} uptake activity, the reaction mixture contained 500 μM EGTA and various amounts of Ca^{2+} To provide the desired range of free Ca^{2+} concentration (from *p*Ca 5.5–7.2). ATP-dependent Ca^{2+} uptake (nmol mg^{-1} min^{-1}) was defined as the difference between the $^{45}Ca^{2+}$ retained in the filters following incubation in the presence and absence of MgATP. The effect of thapsigargin (TG) was tested by adding the compound to a final concentration in the reaction mixture of 0.1 μM at 15 min before the uptake assay was started. $^{45}Ca^{2+}$ uptake and ATPase activity assays were performed at least four times in triplicate.

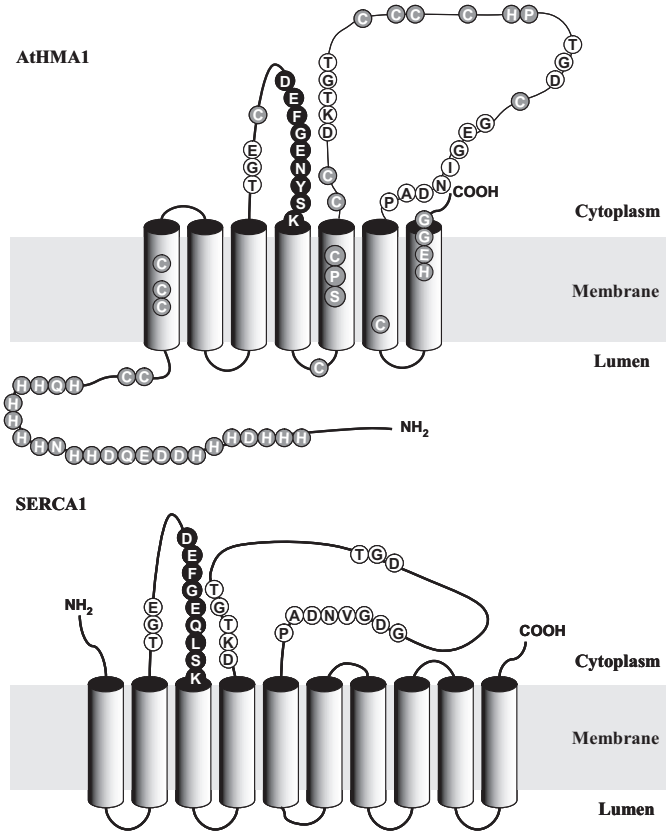

FIGURE 1. **Similarities and differences between AtHMA1 and SERCA1.** Schematic representation of the primary structure and membrane topology of AtHMA1, a heavy-metal pump of the P_{IB}-ATPase family (*top*), and SERCA1, a calcium pump of the P_{IIA}-ATPase family (*bottom*).

RESULTS

Growth Inhibition of Δpmr1 and K616 on Ca^{2+}-deficient Media Is Overcome by the Expression of AtHMA1—Fig. 1 shows a comparison between AtHMA1 and SERCA1. Like all P-type ATPases, both enzymes are transmembrane proteins. SERCA1 possesses ten transmembrane helices, like the vast majority of characterized Ca^{2+}-ATPases. AtHMA1, instead, has seven predicted transmembrane helices (according to the topology prediction software ARAMEMNON). This differs from the characteristic eight predicted transmembrane helices presented in the rest of plant metal-ATPases recruited in the P_{IB}-ATPase subfamily (2).

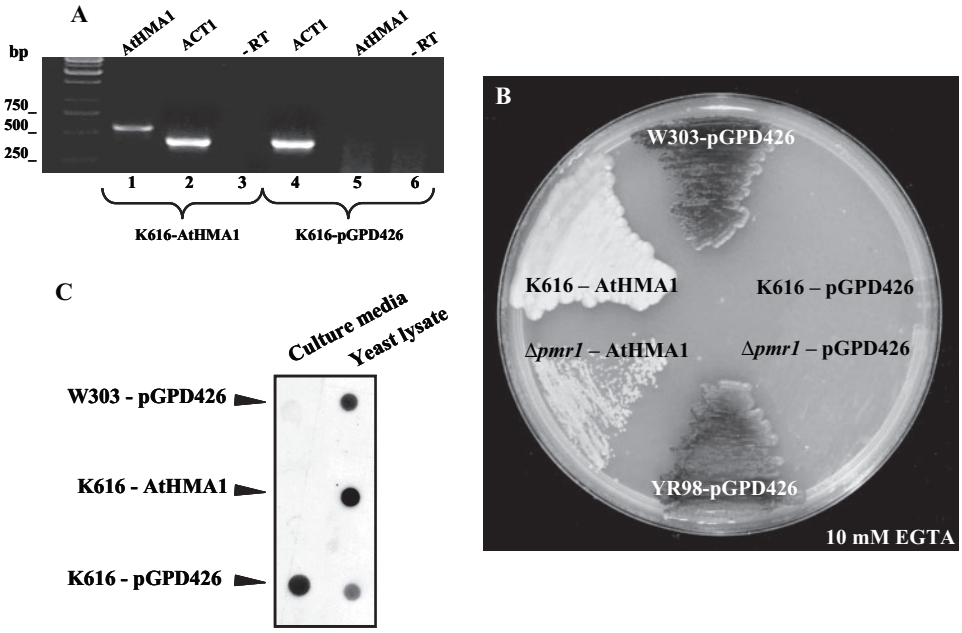

FIGURE 2. **Yeast mutants defective in Ca^{2+} transport are functionally complemented by AtHMA1.** *A*, AtHMA1 expression in transformed yeast strains was verified by RT-PCR as described under "Experimental Procedures." This figure shows RT-PCR performed in samples obtained from K616 cells transformed with either the empty vector (pGPD426) or vector carrying full-length cDNA of AtHMA1. Amplification of a 565-bp fragment corresponding to AtHMA1 was obtained from reactions performed with samples of complemented yeast (*lane 1*). AtHMA1 expression was not detected in control yeast sample (*lane 5*). A −RT control was included to check for contamination with DNA in the crude RNA preparations (*lanes 3* and *6*). ACT1 cDNA was used as an internal control (*lanes 2* and *4*). *B*, lethality of Ca^{2+} transport-deficient yeast strains in Ca^{2+} depleted media was reverted by the expression of AtHMA1. Yeast mutants K616 and Δ*pmr1* transformed with AtHMA1 and pGPD426 were streaked onto selective growth plates containing 10 mM EGTA. Wild-type strains W303 and YR98 transformed with pGPD426 were used as controls. *C*, AtHMA1 abolished the characteristic missorting of CPY displayed by K616 mutant. A dot-blot assay undertaken with an anti-CPY antibody was performed with samples of culture media and yeast lysate obtained from K616 cells transformed with pGPD426 or with AtHMA1. Wild-type cells (W303) were used as control.

On the other hand, AtHMA1 and SERCA1 share the highly conserved Asp in the signature sequence DKTGT that is phosphorylated during the catalytic cycle of P-type ATPases (1, 27, 28). Other common features of P-type ATPases are slightly modified in AtHMA1. For example, the transduction domain TGES (29) in AtHMA1 is TGE*X*. The GDG*X*ND*X*P and TGD motifs involved in ATP binding (27, 28, 30–33) in AtHMA1 are GEGINDAP and TGD, respectively. AtHMA1 also presents motifs involved in heavy metal sensing, binding, and transport. These include several C and CC pairs (34–36), a poly-H domain located at the amino terminus, an HP dipeptide (11, 12, 35, 37), the site SPC essential for metal transport, and a HEGG motif (11, 12, 14). It is noteworthy that AtHMA1, as a heavy metal pump, possesses the signature sequence DEFGENYSK (*black circles*), which is very similar to the DEFGEQLSK sequence involved in the inhibitory effect of thapsigargin in SERCA-type Ca^{2+} pumps (6, 38).

To determine whether AtHMA1 plays a role in Ca^{2+} homeostasis, we performed functional complementation assays using mutant yeast deficient in Ca^{2+} transport. Heterologous expression of the complete AtHMA1 cDNA was performed under the control of the glyceraldehyde-3-phosphate dehydrogenase gene (GPD) promoter (39) and was verified using RT-PCR (Fig. 2*A*). Fig. 2*B* shows that parental wild-type yeast strains YR98 and W303 grew normally on media containing 10 mM EGTA. As demonstrated previously (26), Δ*pmr1*, a strain in which the secretory pathway Ca^{2+}-ATPase PMR1 is disrupted (40), was unable to grow in media depleted of Ca^{2+} in cells transformed with the empty vector. When this mutant was transformed with pGPD426-AtHMA1, growth on Ca^{2+}-deficient medium was restored. AtHMA1 expression also complemented the Ca^{2+} depletion sensitivity of the triple mutant K616, which lacks both endogenous Ca^{2+} pumps (PMR1 and PMC1) and calcineurin (CNB1) function (19, 41, 42). Similar to Δ*pmr1*, K616 transformed with the empty vector did not grow on a medium containing very low Ca^{2+} (10 mM EGTA). Nevertheless, the triple mutant transformed with pGPD426-AtHMA1 became tolerant of this condition (Fig. 2*B*), supporting the hypothesis that AtHMA1 encodes a functional Ca^{2+} pump.

AtHMA1 Reverts the Missorting Phenotype Displayed by K616—Given that yeast mutants lacking the secretory pathway Ca^{2+}-ATPase PMR1 partially secrete carboxypeptidase Y, an enzyme normally destined to the vacuole (40), we evaluated the effect of AtHMA1 expression on this characteristic phenotype. CPY secreted due to missorting was detected using a monoclonal anti-CPY antibody. CPY was detected in a culture media sample recovered from K616 cells transformed with the empty vector as shown in Fig. 2*C*. However, CPY was not detected in the culture media of K616 cells transformed with pGPD426-AtHMA1. In both cases, intracellular accumulation of CPY was verified in cell lysates. The wild-type strain was used as a negative control, as CPY is not secreted under normal conditions (26).

Active Ca^{2+} Transport in K616 Membrane Vesicles Is Increased upon Expression of AtHMA1 and Is Inhibited by TG—Our results indicate that mutant yeast strains K616 and Δ*pmr1* are functionally complemented by AtHMA1. To determine whether this is due to a direct increase in Ca^{2+} transport, we assayed *in vitro* ATP-dependent $^{45}Ca^{2+}$ uptake into intracellular membrane vesicles isolated from K616 cells transformed with the empty vector or a vector carrying AtHMA1 cDNA. As expected, K616 membranes exhibited no significant increase in total $^{45}Ca^{2+}$ accumulation after ATP was added to the reaction medium (Fig. 3*A*). We subsequently analyzed Ca^{2+} uptake into membranes harvested from K616 cells expressing AtHMA1. $^{45}Ca^{2+}$ accumulation in these vesicles was stimulated by ATP and was ~2-fold higher than the $^{45}Ca^{2+}$ retained in membranes of the K616 mutant (Fig. 3*A*). The kinetic parameters of Ca^{2+} uptake activity displayed by AtHMA1 were determined by measuring the initial rates of $^{45}Ca^{2+}$ uptake at different free

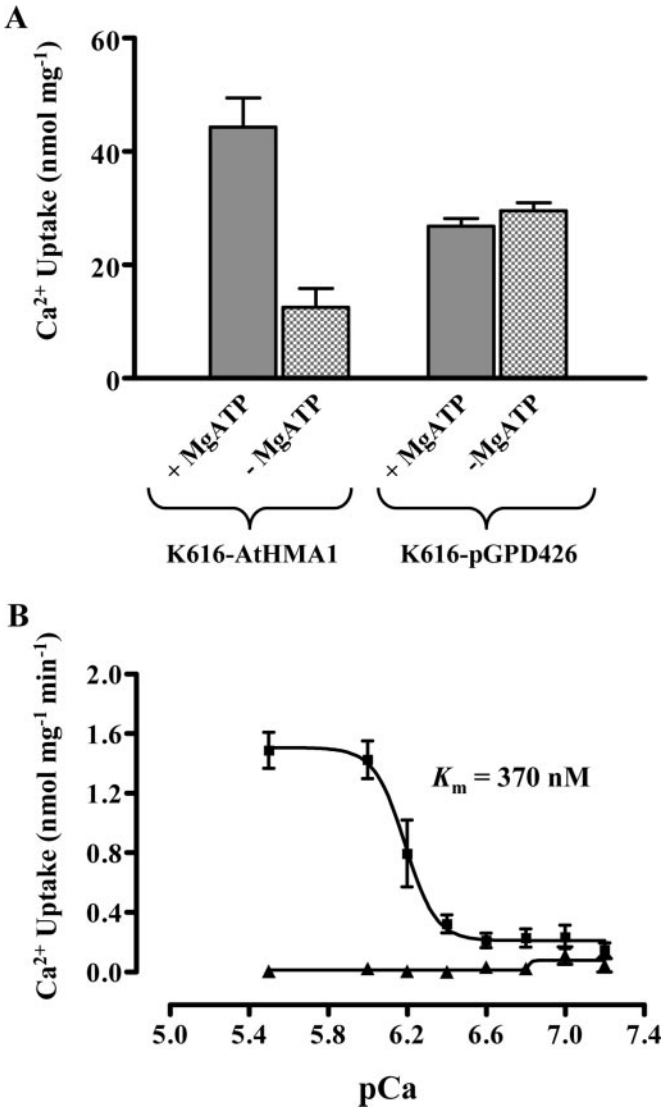

FIGURE 3. **AtHMA1-mediated active Ca^{2+} uptake in yeast.** *A*, Ca^{2+} uptake in K616 cells is increased upon expression of AtHMA1. Membrane fractions obtained from K616-AtHMA1 and K616-pGPD426 cells were incubated for 10 min in a reaction mixture containing 1 μM free $^{45}Ca^{2+}$ (estimated with the WinMaxC 2.05 computer program; Chris Patton, Hopkins Marine Station, Stanford University, CA) and ATP and $MgCl_2$ to final concentrations of 2 and 3 mM, respectively. Ca^{2+} uptake by membranes was assayed measuring $^{45}Ca^{2+}$ accumulation using the filtration method described under "Experimental Procedures." *B*, Ca^{2+} dependence of active Ca^{2+} uptake. Initial rates of Ca^{2+} uptake measured in membranes of K616-AtHMA1 cells (■) and membranes of K616-pGPD426 (▲) at different free Ca^{2+} concentrations. The experimental points for K616-pGDP426 were fitted by a nonlinear fitting program (GraphPad Prism 5, GraphPad Software, Inc., San Diego). An apparent K_m value of 0.37 μM (*p*Ca 6.43) was obtained from interpolation in nonlinear fit. Experiments were performed at least four times in triplicate. Values are mean ± S.E.

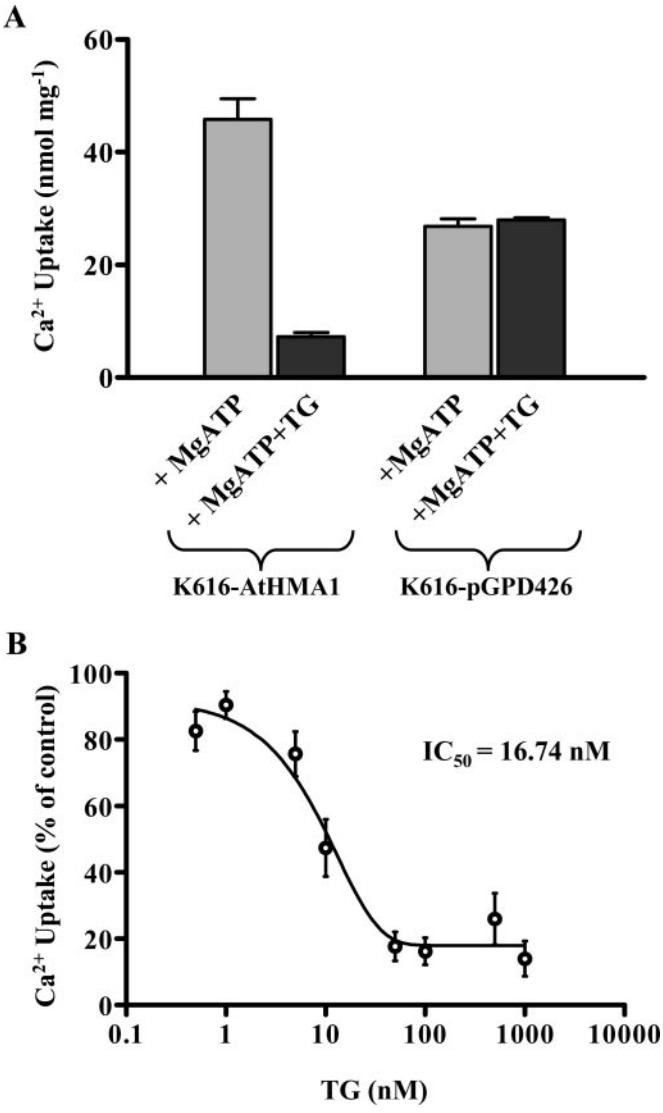

FIGURE 4. **AtHMA1 is inhibited by TG.** *A*, the effect of TG was tested on Ca^{2+} uptake activity of membrane fractions obtained from K616-AtHMA1 and K616-pGPD426 cells by adding 100 nM TG to the reaction mixture. *B*, determination of thapsigargin IC_{50} = 16.74 nM (concentration that causes 50% inhibition of Ca^{2+} uptake activity) for AtHMA1 was performed in uptake assays with a constant free $^{45}Ca^{2+}$ concentration (*p*Ca = 6) and varied TG concentrations in the reaction mixture.

Ca^{2+} concentrations (Fig. 3*B*). The calculated apparent K_m for Ca^{2+} was 370 nM (*p*Ca 6.43), and the maximum rate of Ca^{2+} uptake was 1.53 nmol mg^{-1} min^{-1}. This demonstrates that AtHMA1 functions as a high affinity Ca^{2+}-ATPase in yeast. As described above, AtHMA1 has an S5 segment very similar to the S3 segment involved in determining sensitivity to TG in SERCA type Ca^{2+} pumps (6, 38). The ATP-dependent Ca^{2+} uptake exhibited by the complemented mutant was reduced by 84% in the presence of 100 nM TG (Fig. 4*A*). In contrast, TG did

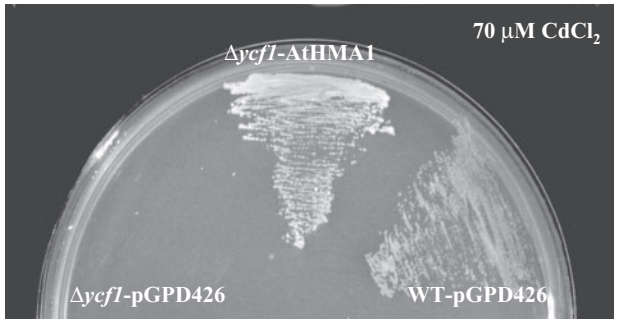

FIGURE 5. **AtHMA1 functionally complements the cadmium-hypersensitive mutant Δycf1.** Functional complementation of Δ*ycf1* by AtHMA1 was performed in solid media assays. Δ*ycf1*-pGPD426 and Δ*ycf1*-AtHMA1 were streaked onto selective growth plates lacking uracil and containing 70 μM CdCl2. Wild-type strain DTY165 was used as control.

TABLE 1

Generation times (G_t) of *S. cerevisiae* strains transformed with the empty pGPD426 vector or a vector carrying AtHMA1 cDNA

G_t was measured during the exponential growth phase on selective media supplemented with increasing $CdCl_2$ concentrations. The rate of exponential growth of yeast cultures was expressed as generation time in hours (h), *i.e.* the doubling time of each yeast population. Values are means of triplicate experiments ± S.E.

	Generation time				
	0 μM Cd	70 μM Cd	100 μM Cd	150 μM Cd	200 μM Cd
			(h)		
WT-pGPD426	4.227 ± 0.077	9.476 ± 1.737	38.983 ± 3.654	101.610 ± 9.140	89.460 ± 22.410
Δ*ycf1*-pGPD426	4.776 ± 0.083	69.765 ± 0.225	75.760 ± 0.550	313.400 ± 8.100	336.550 ± 26.950
Δ*ycf1*-AtHMA1	12.613 ± 0.421	15.313 ± 0.841	13.767 ± 0.152	14.467 ± 1.081	14.193 ± 0.979

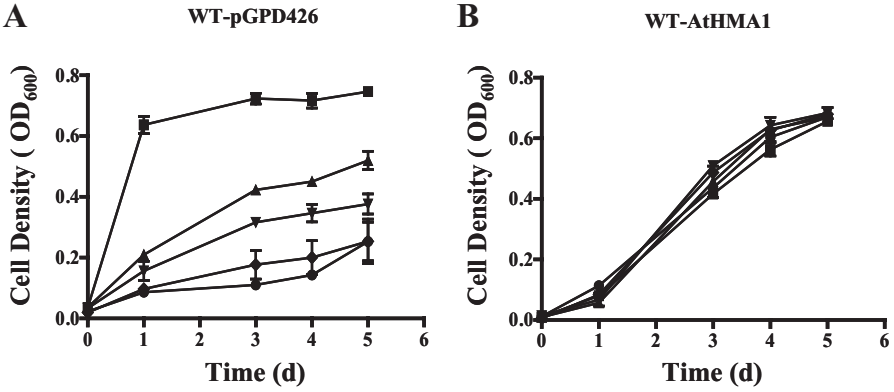

FIGURE 6. **AtHMA1 enhances cadmium tolerance of wild-type yeast.** Growth curves of WT (W303) transformed with empty pGPD426 vector (*A*) and WT (W303) expressing AtHMA1 (*B*). Yeast were grown at 30 °C in selective liquid media supplemented with 0 μM ■, 70 μM ▲, 100 μM ▼, 150 μM ◆, and 200 μM ● $CdCl_2$. Cell densities ($A_{600\ nm}$) were followed for 5 days. Experiments were performed in triplicate, and values are means ± S.E.

not affect calcium uptake in empty vector-transformed yeast. To further characterize the effects of this inhibitor on AtHMA1, we studied the concentration dependence of transport inhibition by TG. The results showed that the apparent inhibitor concentration causing 50% inhibition (IC_{50}) for TG was 16.74 nM (Fig. 4*B*).

AtHMA1 Expression Reverts the Cadmium-hypersensitive Phenotype Displayed by the Mutant Yeast Δycf1 and Confers High Cadmium Tolerance onto Wild-type Yeast—Although AtHMA1 belongs to the subclass of $Zn^{2+}/Co^{2+}/Cd^{2+}/Pb^{2+}$ P_{IB}-ATPases (2), there is no substantial evidence that AtHMA1 plays a role in cadmium transport or detoxification. To elucidate the role of AtHMA1 in cadmium transport, we performed functional complementation assays of the cadmium-hypersensitive yeast Δ*ycf1* and tested the effect of AtHMA1 expression on cadmium tolerance of wild-type yeast. Yeast cells were grown on solid media supplemented with 70 μM Cd^{2+} in an effort to evaluate the cadmium sensitivity displayed by Δ*ycf1* transformed with AtHMA1 or empty vector. AtHMA1-expressing cells grew in a manner similar to wild-type cells (Fig. 5). As expected, Δ*ycf1*-pGPD426 cells did not survive in this medium (43). The high Cd^{2+} tolerance of Δ*ycf1* yeast expressing AtHMA1 was confirmed by growing transformed cells in liquid growth medium supplemented with increasing concentrations of this heavy metal. The first remarkable effect of AtHMA1 expression in Δ*ycf1* cells was an increase in the generation time (G_t) (the doubling time of each yeast population) under control conditions compared with the growth exhibited by Δ*ycf1* and the wild-type strain (DTY165) (Table 1). Nevertheless, at higher concentrations of cadmium (from 100 to 200 μM Cd^{2+}), Δ*ycf1* cells expressing AtHMA1 grew faster than the control strains. This feature is reflected in a decrease of G_t compared with control strains (Table 1). To determine whether AtHMA1 could also enhance the intrinsic cadmium tolerance displayed by wild-type yeast, we compared growth on high Cd^{2+} over 5 days in empty vector-transformed WT (W303) cells (WT-pGPD426) and AtHMA1-expressing WT cells (WT-AtHMA1). WT-pGPD426 was able to grow in all Cd^{2+} concentrations assayed (from 70 to 200 μM) (Fig. 6*A*), but the G_t increased as the heavy metal concentration increased (Table 2). Under control conditions (*i.e.* no cadmium added), WT-AtHMA1 grew slower than WT-pGPD426 (Fig. 6*B*, Table 2). This effect is very similar to that observed in Δ*ycf1* cells expressing AtHMA1 (Table 1). Interestingly, the enhancing effect of AtHMA1 expression over the cadmium tolerance of WT yeast became more evident when Cd^{2+} reached toxic levels for empty vector-transformed WT yeast (up to 100 μM). WT-AtHMA1 cells grew faster than WT-pGPD426 in all of the Cd^{2+} concentrations assayed. Table 2 shows that the generation time for WT-AtHMA1 was similar for all treatments.

Cadmium, Cobalt, Copper, and Zinc Activate AtHMA1 ATPase, and Its Expression Enhances Tolerance to These Metals in Yeast—Our results indicate that AtHMA1 participates in cadmium detoxification in yeast. To confirm that AtHMA1 is a Cd^{2+}-ATPase, we performed a biochemical characterization of its heavy metal specificity after expression in Δ*ycf1* yeast. Microsomal membranes were analyzed for heavy metal-activated ATPase activity. The ATPase measurements indicate that AtHMA1-transformed yeast is activated more by Cd^{2+} (6-fold) than yeast transformed with empty vector (Fig. 7*A*). This coincides with the results obtained in the complementation assay of Δ*ycf1*. Zn^{2+} (15-fold), Cu^{+} (13-fold), and to a lesser extent Co^{2+} (3-fold) also stimulated ATPase activity.

Given that AtHMA1 has been classified in the group of $Zn^{2+}/Co^{2+}/Cd^{2+}/Pb^{2+}$ ATPases (2), our evidence indicates

TABLE 2

Generation times (G_t) of wild-type (W303) yeast transformed with the empty vector or a vector carrying AtHMA1 cDNA

G_t was measured during the exponential growth phase on selective media supplemented with increasing $CdCl_2$ concentrations. Values are means of triplicate experiments ± S.E.

	Generation time				
	0 μM Cd	70 μM Cd	100 μM Cd	150 μM Cd	200 μM Cd
			(h)		
WT-pGPD426	5.764 ± 0.640	9.633 ± 1.185	60.640 ± 5.043	458.517 ± 16.097	631.665 ± 27.036
WT-AtHMA1	30.097 ± 0.048	28.093 ± 0.664	15.660 ± 1.983	17.280 ± 0.592	31.213 ± 0.292

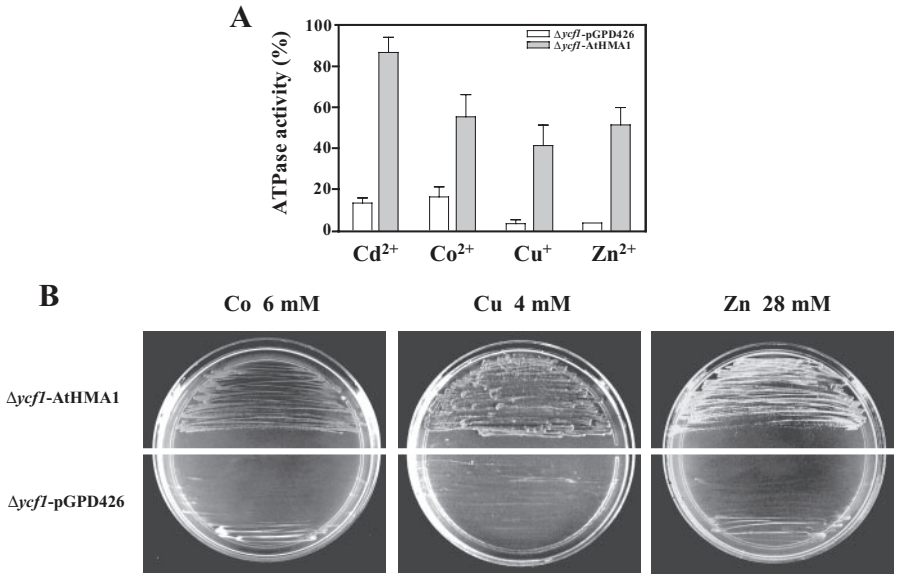

FIGURE 7. **ATPase activity of AtHMA1 is activated by cadmium, copper, zinc, and cobalt, and its expression enhances metal tolerance in yeast.** *A*, metal-activated ATPase activity of AtHMA1 was determined in membranes from Δ*ycf1*-pGPD426 cells (*white bars*) and Δ*ycf1*-AtHMA1 cells (*gray bars*). *B*, growth of Δ*ycf1*-pGPD426 and Δ*ycf1*-AtHMA1 cells on solid selective medium in the presence of 6 mM $CoCl_2$, 4 mM $CuSO_4$, or 28 mM $ZnCl_2$. Plates were incubated for 5 days at 30 °C.

that AtHMA1 transports Ca^{2+} with high affinity but also participates in Cd^{2+} detoxification. Our research also suggests that its ATPase activity could also be activated by Cd^{2+}, Zn^{2+}, Cu^{+}, and Co^{2+}. To confirm that AtHMA1 plays a role in zinc, copper, and cobalt homeostasis, Δ*ycf1* cells expressing AtHMA1 were used to test its ability to confer tolerance onto toxic levels of these heavy metals. Fig. 7*B* shows that Δ*ycf1* cells transformed with empty vector (Δ*ycf1*-pGPD426) exhibited poor growth on solid media containing 6 mM $CoCl_2$, 4 mM $CuSO_4$, or 28 mM $ZnCl_2$. However, AtHMA1-expressing cells (Δ*ycf1*-AtHMA1) grew normally under these conditions.

DISCUSSION

AtHMA1 Functions as a Thapsigargin-sensitive Ca^{2+} Pump in Yeast—Because TG is a plant-derived compound and there are no molecularly characterized TG-sensitive Ca^{2+} pumps, it has been proposed that plants may have developed insensitivity to this compound (23). Neither the members of the plant Ca^{2+}-ATPase family in *A. thaliana* nor calcium pumps of other plant species possess the characteristic conserved motif DEFGE*XX*SK associated with the binding and highly specific inhibition of TG. AtHMA1 is the only plant P-type ATPase among the subclass of the heavy metal pumps that possesses this particular motif in its sequence.

Interestingly, AtHMA1 is able to transport calcium with an affinity similar to other Ca^{2+}-ATPases described in *Arabidopsis* (23). Moreover, the IC_{50} measured was 16.74 nM, which is close to the range of sensitivity of SERCA-ATPases (44). In *Arabidopsis*, calcium pumps that exhibit homology to SERCA-ATPases are classified in the P_{IIA} subfamily of P-type ATPases (2). The four members of this subfamily transport calcium through the membrane of organelles or the plasma membrane (1, 2). In addition to AtHMA1, some members of the P_{IIA} subfamily could also transport transition metals such as manganese and zinc (45). This demonstrates the importance of functional characterization for classification purposes in addition to grouping P-type ATPases based on structural similarities.

AtHMA1 decreases sensitivity to a medium with low calcium for two calcium transport-deficient yeast mutants (Δ*pmr1* and K616). In addition, expression of AtHMA1 fully restores the CPY missorting phenotype of K616 (26). On the other hand, it is likely that AtHMA1 expressed in Δ*pmr1* restores the transport of calcium into the lumen of the Golgi apparatus, the organelle where calcium ions are needed for normal protein processing and sorting in yeast (26, 40).

AtHMA1 Participates in Heavy Metal Detoxification in Yeast—Cadmium is a nonessential element and in fact is toxic for cells. Functional expression of AtHMA1 phenotypically complements a cadmium-hypersensitive yeast strain and, interestingly, also confers an extraordinary cadmium tolerance onto wild-type yeast. In addition, cadmium significantly stimulates the ATPase activity of AtHMA1. It is possible that expression of AtHMA1 in *S. cerevisiae* may help to concentrate cadmium in organelles or mediate its extrusion to the extracellular medium, overcoming the stress produced by elevated concentrations of cadmium.

A role for AtHMA1 in copper transport in plants has been proposed by Seigneurin-Berny *et al.* (14). They demonstrated through yeast expression that AtHMA1 is involved in both zinc and copper homeostasis. Furthermore, they have provided evidence that AtHMA1 is located in the chloroplast envelope, and measurements of ATPase activity in purified chloroplast enve-

lope membranes demonstrated that AtHMA1 activity is stimulated by copper but not by zinc, cobalt, iron, manganese, or silver (14). Our results show some differences. One explanation for this discrepancy is that Seigneurin-Berny *et al.* (14) used a truncated version of AtHMA1 (where the transit peptide of the protein was deleted) for the heterologous expression and functional studies in yeast. In contrast, we were able to detect protein activity using full-length cDNA expression in yeast. Moreover, we found that yeast cells expressing AtHMA1 are able to grow faster than those transformed with the empty vector in a growth medium supplemented with high copper. These data demonstrated that full-length AtHMA1 increases metal tolerance in yeast. We also provided evidence of participation of AtHMA1 in cadmium, zinc, and cobalt detoxification.

It also has been suggested that AtHMA1 may be involved in zinc homeostasis (13). The evidence supporting this hypothesis is based on studies showing that an *Arabidopsis* disruption mutant of AtHMA1 is sensitive to high concentrations of zinc. This is consistent with the presence of a long His stretch in the sequence of AtHMA1, which is reminiscent of the poly(His) sequence that has proved to be involved in zinc transport in other species (36, 46, 47). Despite this characteristic sequence, no direct evidence of AtHMA1 participation in zinc transport had been obtained. We demonstrated that growth in a medium with high concentrations of zinc is faster in cells transformed with AtHMA1 than in cells transformed with the empty vector. This suggests that AtHMA1 could function as a zinc transporter. Furthermore, ATPase activity of AtHMA1 was highly stimulated by zinc, which provides additional support for the theory that this protein does transport this heavy metal.

There are structural differences between AtHMA1 and the other members of the P_{IB} family. One unique characteristic that has been used to infer its function is its homology with CoaT. CoaT is a P-type ATPase from *Synechocystis* PCC6803, which appears to confer Co^{2+} tolerance onto this organism (48). Based on this homology, it has been suggested that AtHMA1 may play a significant role in cobalt homeostasis in *Arabidopsis* (24). Here we confirm that AtHMA1 participates in cobalt detoxification in yeast. Yeast cells transformed with AtHMA1 grow faster than empty vector-transformed cells when they are grown in a medium supplemented with high cobalt. This result suggests that AtHMA1 could participate in the transport of this trace element. Cobalt (as well as cadmium, copper, and zinc) also stimulated the ATPase activity of AtHMA1, providing further evidence that this pump is able to transport Co^{2+}.

Functional Expression of AtHMA1 in Yeast—Recent data suggest that AtHMA1 is an intrinsic protein of the chloroplast membrane envelope in *Arabidopsis*. This raises questions regarding the way in which AtHMA1 manages to complement defective yeast strains that lack ion transporters in other compartments such as the vacuole and the Golgi apparatus. The yeast cells provide a convenient system for uptake studies using plant transporters and represent a useful tool for studying their transport mechanisms and specificity. However, the activity of these transporters in plants may be modulated by interactions with proteins that are absent in yeast, and the expression of the genes might be developmentally or environmentally regulated, which may contribute to their specific functions (48). This is not the first example of transporters that appears to be localized differently in yeast and plants (49–51). Triose phosphate translocators in the chloroplast membrane are found in endoplasmic reticulum membranes upon expression in yeast (52). This suggests that AtHMA1 could be translated into the endoplasmic reticulum and be present in organelles of the yeast secretory pathway such as the endoplasmic reticulum, Golgi, and vacuole. Thus functional AtHMA1 would be compensating for a failure in a specific organelle, explaining why AtHMA1 was able to complement the Δ*pmr1*, K616, and Δ*ycf1* yeast mutants. Based on these results, we suggest that AtHMA1 has diverse specificity that might allow it to have various *in planta* roles related to metal and Ca^{2+} homeostasis. The role of AtHMA1 as a multimetal transporter is beginning to be unraveled, and further studies are needed to elucidate its relevance for ionic homeostasis in *A. thaliana.*

Acknowledgments—We thank Drs. Hans Rudolph, Kyle Cunningham, and Dennis Thiele for providing the Δpmr1, K616, and Δycf1 mutant strains, respectively. We also thank Dr. Michael Handford and members of the Faculty of Sciences' Cellular Physiology Laboratory, University of Chile, for helpful discussions and Dr. Lindsey Nicholson for reading the manuscript and offering suggestions and observations.

REFERENCES

1. Axelsen, K. B., and Palmgren, M. G. (1998) *J. Mol. Evol.* **46,** 84–101
2. Axelsen, K. B., and Palmgren, M. G. (2001) *Plant Physiol.* **126,** 696–706
3. Colangelo, E. P., and Guerinot M. L. (2006) *Curr. Opin. Plant Biol.* **9,** 322–330
4. Geisler, M., Axelsen, K. B., Harper, J. F., and Palmgren, M. G. (2000) *Biochim. Biophys. Acta* **1465,** 52–78
5. Zhang, Z., Sumbilla, C., Lewis, D., and Inesi, G. (1993) *FEBS Lett.* **335,** 261–264
6. Zhong, L., and Inesi, G. (1998) *J. Biol. Chem.* **273,** 12994–12998
7. Xu, Ch., Ma, H., Inesi, G., Al-Shawi, M. K., and Toyoshima, C. (2004) *J. Biol. Chem.* **279,** 17973–17979
8. Toyoshima, C., Nakasako, M., Nomura, H., and Ogawa, H. (2000) *Nature* **405,** 647–655
9. Stokes, D., and Green, N. M. (2003) *Annu. Rev. Biophys. Biomol. Struct.* **32,** 445–468
10. Cobbett, C. S., Hussain, D., and Haydon, M. J. (2003) *New Phytol.* **159,** 315–321
11. Williams, L., and Mills, R. (2005) *Trends Plant Sci.* **10,** 1360–1385
12. Argüello, J. M. (2003) *J. Membr. Biol.* **195,** 93–108
13. Higuchi, M., and Sonoike, K. (2005) in *Photosynthesis: Fundamental Aspects to Global Perspectives* (van der Est, A., and Bruce, D., eds) pp. 716–718, International Society of Photosynthesis
14. Seigneurin-Berny, D., Gravot, A., Auroy, P., Mazard, C., Kraut, A., Finazzi, G., Grunwald, D., Rappaport, F., Vavasseur, A., Joyard, J., Richaud, P., and Rolland, N. (2006) *J. Biol. Chem.* **281,** 2882–2892
15. Seki, M., Narusaka, M., Kamiya, A., Ishida, J., Satou, M., Sakurai, T., Nakajima, M., Enju, A., Akiyama, K., Oono, Y., Muramatsu, M., Hayashizaki, Y., Kawai, J., Carnicini, P., Itoh, M., Ishii, Y., Arakawa, T., Shibata, K., Shinagawa, A., and Shinozaki, K. (2002) *Science* **296,** 141–145
16. Seki, M., Carnicini, P., Nishiyama, Y., Hayashizaki, Y., and Shinozaki, K. (1998) *Plant J.* **15,** 707–720
17. Mumberg, D., Muller, R., and Funk, M. (1995) *Gene* **156,** 119–122
18. Sambrook, J., Fritsch, E. F., and Maniatis, T. (eds) (1989) *Molecular Cloning: A Laboratory Manual*, 2nd Ed., Cold Spring Harbor Laboratory, Cold Spring Harbor, NY

19. Liang, F., Cunningham, K. W., Harper, J. F., and Sze, H. (1997) *Proc. Natl. Acad. Sci. U. S. A.* **94,** 8579–8584
20. Gietz, D., St Jean, A., Woods, R. A., and Schiestl, R. H. (1992) *Nucleic Acids Res.* **20,** 1425
21. Chomczynski, P., and Sacchi, N. (1987) *Anal. Biochem.* **162,** 156–159
22. Del Aguila, E. M., Dutra, M. B., Silva, J. T., and Paschoalin, V. M. F. (2005) *BMC Mol. Biol.* **6,** 9
23. Liang, F., and Sze, H. (1998) *Plant Physiol.* **118,** 817–825
24. Eren, E., and Argüello, J. M. (2004) *Plant Physiol.* **136,** 3712–3723
25. Lanzetta, P. A., Alvarez, L. J., Reinach, P. S., and Candia, O. A. (1979) *Anal. Bichem.* **100,** 95–97
26. Durr, G., Strayle, J., Plemper, R., Elbs, S., Klee, S. K., Catty, P., Wolf, D. H., and Rudolph, H. K. (1998) *Mol. Biol. Cell* **9,** 1149–1162
27. Lutsenko, S., and Kaplan, J. H. (1995) *Biochemistry* **34,** 15607–15613
28. Aravind, L., Galperin, M. Y., and Koonin, E. V. (1998) *Trends Biochem. Sci.* **23,** 127–129
29. Andersen, J. P., and Vilsen, B. (1995) *FEBS Lett.* **359,** 101–106
30. Toyoshima, C., and Inesi, G. (2004) *Annun. Rev. Biochem.* **73,** 269–292
31. Jensen, A. M., Sørensen, T. L., Olesen, C., Møller, J. V., and Nissen, P. (2006) *EMBO J.* **25,** 2305–2314
32. Efremov, R. G., Kosinsky, Y. A., Nolde, D. E., Tsivkovskii, R., Arseniev, A. S., and Lutsenko, S. (2004) *Biochem. J.* **382,** 293–305
33. Savinsky, M. H., Mandal, A. K., Argüello, J. M., and Rosenzweig, A. C. (2006) *J. Biol. Chem.* **281,** 11161–11166
34. Solioz, M., and Vulpe, C. (1996) *Trends Biochem. Sci.* **21,** 237–241
35. Eren, E., Kennedy, D. C., Maroney, M. J., and Argüello, J. M. (2006) *J. Biol. Chem.* **281,** 33881–33891
36. Mills, R. F., Francini, A., Ferreira da Rocha, P. S. C., Baccarini, P. J., Aylett, M., Krijger, G. C., and Williams, L. E. (2005) *FEBS Lett.* **579,** 783–791
37. Verret, F., Gravot, A., Auroy, P., Preveral, S., Forestier, C., Vavasseur, A., and Richaud, P. (2005) *FEBS Lett.* **579,** 1515–1522
38. Sagara, Y., and Inesi, G. (1991) *J. Biol. Chem.* **266,** 13503–13506
39. Bitter, G. A., and Egan, K. M. (1984) *Gene* **32,** 263–274
40. Antebi, A., and Fink, G. (1992) *Mol. Biol. Cell* **3,** 633–654
41. Cunningham, K. W., and Fink, G. R. (1994) *J. Cell Biol.* **124,** 351–363
42. Harper, J. F., Hong, B., Hwang, I., Guo, H. Q., Stoddard, R., Huang, J. F., Palmgren M. G., and Sze, H. A. (1998) *J. Biol. Chem.* **273,** 1099–1106
43. Gravot, A., Lieutaud, A., Verret, F., Auroy, P., Vavasseur, and A., Richaud, P. (2004) *FEBS Lett.* **561,** 22–28
44. Wootton, L. L., and Michelangeli, F. (2006) *J. Biol. Chem.* **281,** 6970–6976
45. Wu, Z., Liang, F., Hong, B., Young, J. C., Sussman, M. R., and Harper, J. F. (2002) *Plant Physiol.* **130,** 128–137
46. Tong, L., Nakashima, S., Shibasaka, M., Katsuhara, M., and Kasamo, K. (2002) *J. Bacteriol.* **184,** 5027–5035
47. Mills, R. F., Krijger, G. C., Hall, J. L., and Williams, L. E. (2003) *Plant J.* **35,** 164–176
48. Rutherford, J. C., Cavet, J. S., and Robinson, N. J. (1999) *J. Biol. Chem.* **274,** 25827–25832
49. Bassham, D. C., and Raikhel, N. V. (2000) *Plant Physiol.* **122,** 999–1001
50. Apse, M. P., Aharon, G. S., Snedden, W. A., and Blumwald, E. (1999) *Science* **285,** 1256–1258
51. Gaxiola, R. A., Rao, R., Sherman, A., Grisafi, P., Alper, S. L., and Fink, G. R. (1999) *Proc. Natl. Acad. Sci. U. S. A.* **96,** 1480–1485
52. Loddenkötter, B., Kammerer, B., Fischer, K., and Flügge, U. I. (1993) *Proc. Natl. Acad. Sci. U. S. A.* **90,** 2155–2159